



## FORMULATION AND CHARACTERIZATION OF MAGNETIC NANOPARTICLES OF TAMOXIFEN CITRATE

Kalpeshkumar S. Wagh<sup>1\*</sup>, Dr.Namrata Singh<sup>2</sup>

<sup>1\*</sup>Research Scholar, Department of Pharmaceutics, Oriental University, Indore, Madhya Pradesh, India.

<sup>2</sup>Faculty of Pharmacy, Department of Pharmacognosy, Oriental University, Indore, Madhya Pradesh, India.

**\*Corresponding Author:** - Kalpeshkumar S. Wagh

\*Research Scholar, Department of Pharmaceutics, Oriental University, Indore, Madhya Pradesh, India. 453555, E-mail: kalpeshwagh25@gmail.com Mobile No. 07588002726

---

### Abstract:

In this work, iron oxide MNPs was effectively prepared by co-precipitation method that is effortless and facilitates of integrating. The main aim of this method is that a huge measure of NPs can be set up. At that point, these nanoparticles were functionalized with arginine to us for biomedical applications because of their great similarity. The surface functionalization of NPs is obviously worthwhile attributable to shield them from agglomeration and furthermore limit the additional cell cooperation. Additionally, it makes option of biomolecules conceivable. For example, amino acids can be utilized to form with corrosive gatherings of TMX. From that point forward, TMX was formed to NPs by the expansion of EDC and NHS. The morphology and size of them were researched by the TEM. It very well may be seen that these NPs had a round shape with consistency in morphology.

**Keywords:** MNP's, Cancer, Tamoxifen citrate, Breast Cancer, TMX.

### INTRODUCTION:

Cancer has afflicted people for several centuries. It is because of the early research that we hold a greater knowledge of cancer today. The word Cancer is derived from the Greek word Karakinos, for "crab." Cancer [1] can start almost anywhere in the human body, which is made up of trillions of cells. Normally, human cells grow and divide to form new cells as the body needs them. When cells grow old or become damaged, they die, and new cells take their place [2]. When cancer develops, however, this orderly process breaks down. As cells become more and more abnormal, old or damaged cells survive when they should die, and new cells form when they are not needed.

In patients whose cancer expresses an over-abundance of the HER2, protein, a monoclonal antibody known as trastuzumab (Herceptin) is used to block the activity of the HER2 protein in breast cancer cells, slowing their growth. In the advanced cancer setting, trastuzumab [4] use in combination with chemotherapy can both delay cancer growth as well as improve the recipient's survival. More recently, several clinical trials have also confirmed that in the adjuvant setting, i.e. post operative following breast cancer surgery, the use of trastuzumab for up to one year also delays the recurrence of breast cancer and improves survival.

Targeted cancer therapies interfere with cancer cell division [5] (proliferation) and spread in different ways. Many of these therapies focus on proteins that are involved in cell signaling pathways, which form a complex communication system that governs basic cellular functions and activities, such as cell division, cell movement, cell responses to specific external stimuli, and even cell death. By blocking signals that tell cancer cells [6] to grow and divide uncontrollably, targeted cancer therapies can help stop cancer progression and may induce cancer cell death through a process known as apoptosis. Other targeted therapies can cause cancer cell death directly, by specifically inducing apoptosis, or indirectly, by stimulating the immune system to recognize and destroy cancer cells and/or by delivering toxic substances directly to the cancer cells.

### **Nanotechnology:**

The nanotechnology science has helped diagnosis and treatment of diseases by using nanoparticles and development of systematic drug delivery methods [7].

Nanoparticles have high potential in field of diagnosis and treatment of diseases, especially cancer. Using these nanoparticles as factors increasing contrast in conventional imaging method of magnetic resonance and as nano-carriers [8] in modern drug delivery systems.

## **MATERIAL AND METHODS:**

### **Materials:**

Drug tamoxifen citrate procured from Jai Radhe Sales Ahmedabad Gujarat., India,  $\text{FeCl}_3 \cdot 6\text{H}_2\text{O}$  and  $\text{FeCl}_2 \cdot 4\text{H}_2\text{O}$  from Vishnupriya Chemicals Hyderabad Telangana, and Arginine, 1-ethyl-3-[3-(dimethylamino) propyl] carbodiimide (EDC) and N-hydroxysuccinimide (NHS) were obtained from Chemdyes Pvt LTD. Rajkot.

### **Methods:**

#### ***Infrared Spectroscopy Study:***

The medication powder of Tamoxifen Citrate with KBr were ready utilizing water powered pellet press at a pressing factor of 7 to 10 tones. FTIR was checked from 400-4000  $\text{cm}^{-1}$  by utilizing perkin Elmer range GX FTIR [9]. FTIR study was completed exclusively for drug, record FTIR spectra of unadulterated medication and polymer.

#### ***Solubility:***

Solubility is a useful parameter mainly for inadequately solvent medications. Medication solvency was dictated by planning immersed drug arrangements in a water shower and persistently shaken in to mechanical shaker (Remi mechanical shaker, Bombay) up to 24 hrs [10]. Tamoxifen citrate drawn examples were sifted through a channel paper, and tested by UV spectrophotometer.

#### ***Particle Size Measurement:***

Particle size analysis was carried out by malvonometer apparatus and sieve analysis method.

#### ***Melting Point Determination:***

The Melting point of tamoxifen citrate was determined using open capillary method. The fine loaded up with drug powder was set in Thiel's cylinder [11] containing fluid paraffin. The cylinder was warmed and the dissolving purpose of the medication powder was noted. The normal of three qualities was considered as the dissolving purpose of medication.

## **FORMULATION OF TAMOXIFEN CITRATE MAGNETIC NANO-PARTICLES:**

### **Synthesis of Fe-Arg-TMX NPs:**

From the start, 100 mg of Fe-Arg NPs were broken down in DMSO (Dimethyl sulfoxide) (15 mL) and afterward sonicated for 10 min in a sonicating shower at 60°C. From that point forward, free TMX (25 mg), EDC (52.5 mg), and NHS (31.6 mg) were added to this suspension. At that point,

triethylamine was added until the pH arrived at 8.2 and was blended at 37°C in dimness short-term. At last, these nanoparticles were isolated from the fluid arrangement by an outside magnet and washed multiple times with deionized water [12].

### **CHARACTERIZATION OF THE Fe-Arg-TMX NPs:**

#### **Determination of TMX conjugated on the Fe-Arg:**

To evaluation of TMX formed on the Fe-Argnano-particles surface, bright noticeable (UV–Vis) spectroscopy was applied. From the outset, 2.3 mg/mL of Fe-Arg-TMX nanoparticles with 2.3 mg/mL of proteinase K as compound were scattered in PBS (1 mL) and were placed in a dialysis sack (sub-atomic weight 12 kDa). At that point, this sack was submerged in PBS (5 mL) with pH = 7.4. From that point onward, it was hatched on a shaker at 37°C. To acquire the estimation of TMX, UV–Vis spectrophotometer (Thermo Fisher Scientific, Madison, model GENESYS™ 10S) was utilized at a frequency of 235 nm and the outcomes were contrasted and the adjustment bend arranged previously [13].

#### **Drug release study:**

The delivery behavior of TMX from Fe-Arg-TMX nanoparticles was researched by drug discharge study. In this work, the arrival of TMX was assessed with and without protein. Fe-Arg-TMX nanoparticles (5 mg) with proteinase K (5 mg) as chemical were scattered in PBS (2 mL). This suspension was placed in a dialysis pack and drenched in PBS (10 mL) with pH = 5.4. At that point it was hatched at 37°C on a shaker for 5 days [14]. At the particular hatching time, 2 mL of new PBS was put rather than 2 mL of the dialysate arrangement. The delivery study was acted in lysosomal conditions (with a protease in pH = 5.4) and without proteinase K. All outcomes were acquired after multiple times of reiteration of the investigation

### **BIOCOMPATIBILITY FOR TMX MNPs:**

#### **Hemolysis assay:**

Evaluation of biocompatibility with segments of blood is fundamental for biomedical applications. The hemolysis examine was done to consider hemo-compatibility. From the start, the human blood was centrifuged at 3,000 rpm for 10 min. At that point, the supernatant was taken out and 1 mL of the human red platelets (HRBCs) [15-18] was acquired subsequent to washing with sterile PBS. At that point, 1 mL of nanocarrier suspension at high fixation (10 mg/mL) and 1 mL of sterile PBS as negative control and 1 mL of deionized water as sure control were added to weakening of HRBCs. These suspensions were put in a shaker hatchery at 37°C [19]. After 4 hr, the examples were centrifuged at 13,000 rpm for 15 min. At long last, the absorbance of the supernatant was gotten with UV–Vis spectroscopy at 235.0 nm. The accompanying condition was applied for the assurance of percent hemolysis:  $\text{Hemolysis \%} = \frac{A_{\text{sample}} - A_{\text{negative}}}{A_{\text{positive}} - A_{\text{negative}}} \times 100$ ; [20] In this equation,  $A_{\text{positive}}$  and  $A_{\text{negative}}$  are the absorbance of the positive and negative control, respectively. The experiment was replicated three times.

#### **Cell viability assay:**

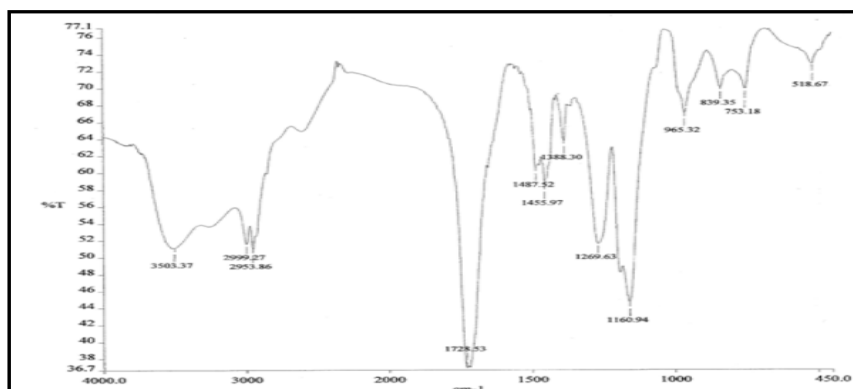
In this investigation, human fibroblast cell line (HFF-2) [21] given by the cancer research center was utilized. The practicality of it within the sight of Fe-Arg nanoparticles and TMX and Fe-Arg-TMX was examined. From the start, the cells were cultivated in 96-well plate for 24 hr at a centralization of 7,000 cells for each well. At that point, different centralizations of Fe-Arg NPs [22] from 100 to 1,200 nM and cells with medium free NPs as control were refined and brooded in a humidified hatchery with 5% CO<sub>2</sub> at 37°C. Subsequent to brooding for 48 and 72 hr, the medium was killed and the MTT arrangement was added to per well for 3 hr in hatchery. At last, the violet formazan gems [23] were broken down with 100 µL of DMSO. In the wake of shaking for 5 min, the absorbance of living cells in Fe-Arg NPs was contrasted and that of the control.

**RESULT AND DISCUSSION:****Table 1:** Physical Parameter of Tamoxifen citrate

Sr. No.	Parameter	Result
1	Color	A white to off white Amorphous powder
2	Odour	Characteristic as per I P 2018
3	Taste	Bitter as per I P 2018

**By Infrared Spectroscopy:**

The Infra-Red ingestion range of the finely ground test in KBr scattering packed into a circle should show maxima just at similar frequencies as that of a comparable readiness of working norm.

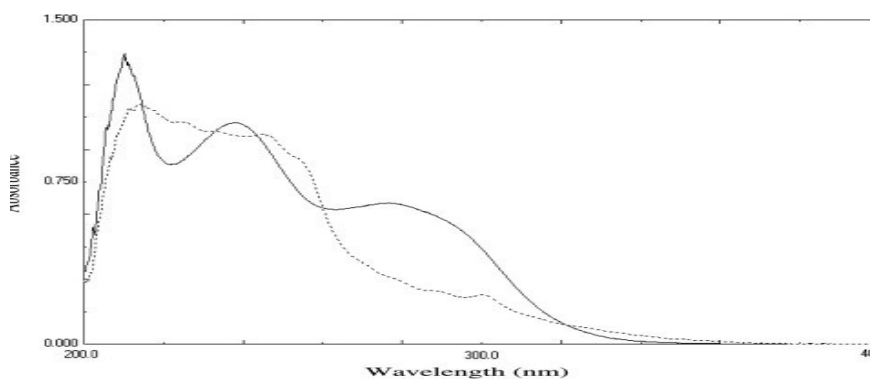
**Figure 1:** IR spectrum of Tamoxifen citrate**Table 2:** Wave number of functional groups of Tamoxifen citrate

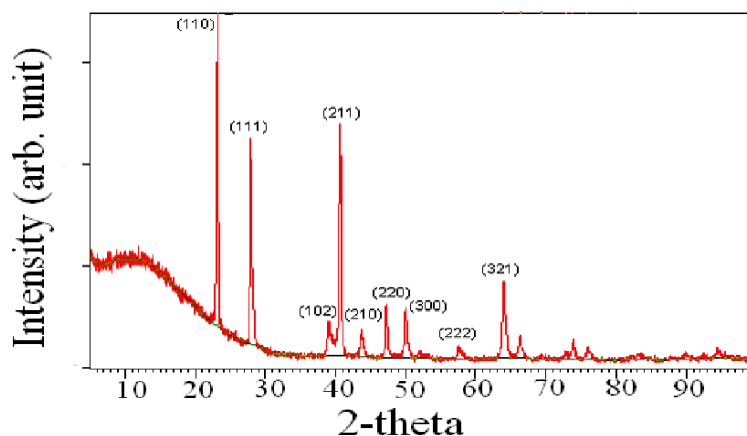
Sr. No.	Wave number	Functional group
1	1551, 1251 $\text{cm}^{-1}$	C=C (Aromatic)
2	1767 $\text{cm}^{-1}$	C=O (ketone)
3	1610 $\text{cm}^{-1}$	C=O (carboxylic acid)
4	1151, 1245 $\text{cm}^{-1}$	C-O (ester/carboxylic acid)
5	3429, 3221 $\text{cm}^{-1}$	O-H (carboxylic acids)

The above peaks can be considered as characteristic peaks of Tamoxifen citrate

**Determination of Analytical Wave length:**

A standard stock arrangement of Tamoxifen citrate in 6.8 phosphate support was readied having a fixation 600  $\mu\text{g/mL}$ . A 5.0 mL part of stock arrangement was additionally weakened Tamoxifen citrate water in a 100.0 mL. volumetric flask up to stamp to get last fixation 30  $\mu\text{g/mL}$ . The standard arrangement of Tamoxifen citrate (30 $\mu\text{g/mL}$ ) was checked in the scope of 400-200 nm in 1.0 cm cell against dissolvable clear and spectra was recorded , the absorbance maxima was seen at 232.0 nm.

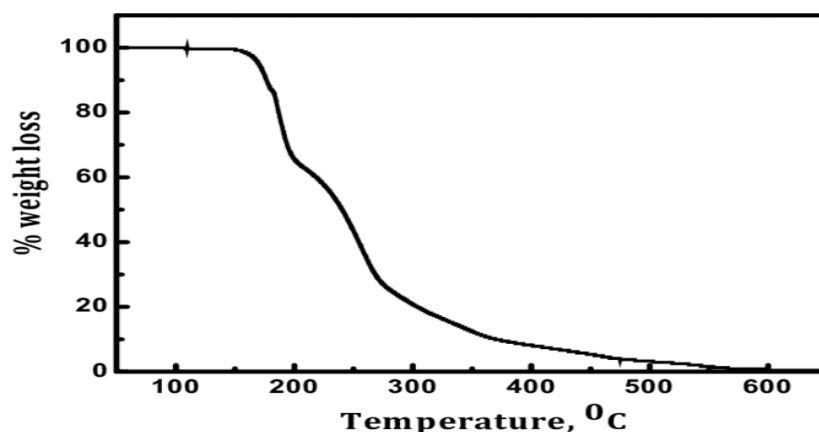
**Figure2:**UV spectrum of Tamoxifen citrate in 6.8 phosphate buffer

**X-ray Diffraction of Tamoxifen citrate Pattern:****Figure 3:** X-ray powder diffraction pattern of Tamoxifen citrate in crystalline form

**DSC Study:** The DSC test was done on Tamoxifen citrate was presented below

**Table No 3:** DSC Study of Tamoxifen citrate

Sl. no	Stage	Temperature
1	Onset	95.16 <sup>0</sup> c
2	Peak	97.17 <sup>0</sup> c
3	End set	99.16 <sup>0</sup> c

**Figure 4:** Thermal Analysis result of Tamoxifen citrate**Structure characterization:**

The XRD example of Fe-Arg NPs was contrasted with its Fe<sub>3</sub>O<sub>4</sub> standard. The relative power and circumstance of all pinnacles of the Fe-Arg NPs compared to its norm, which represented the fruitful amalgamation of iron oxide nanoparticles. The tops in the example of Fe-Arg are at 2θ estimations of 21.24, 36.15, 38.51, 46.20, 56.15, 59.20, and 65.22 which were recorded by their lists (1 1 2), (2 1), (3 2), (4 1), (4 1), (5 0), and (4 0) (hkl) planes.

**Characterization of size and morphology:**

Transmission electron microscopy investigated the size and morphology of Fe-Arg- TMX NPs. The nanoparticles were scattered and had a circular shape without the significant distinction in the morphology. The mean breadth of Fe-Arg-TMX was 32.15 ± 6.45 nm.

**Magnetic properties:**

The attractive highlights of uncovered Fe<sub>3</sub>O<sub>4</sub>, Fe-Arg, and Fe-Arg-TMX, were investigated by VSM.

The charge of the examples was acquired from the immersion esteems when the applied attractive field expanded to 10,000 at RT. The immersion charge (Ms) of  $\text{Fe}_3\text{O}_4$  was  $\sim 76$  emu/g. Ms of Fe-Arg and Fe-Arg-TMX was  $\sim 46$  and  $\sim 22$  emu/g, separately, which was not exactly that of exposed iron.

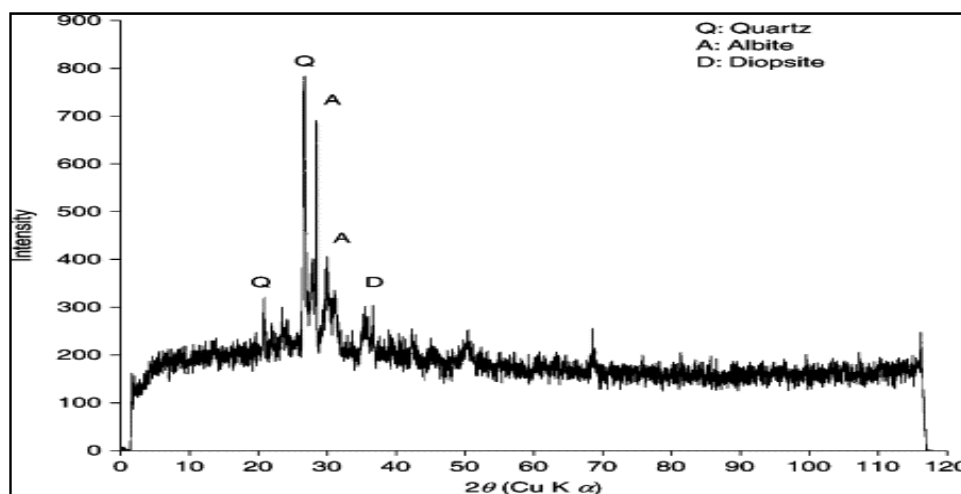


**Figure 5:** XRD pattern of Fe-Arg. XRD, X-ray diffraction

#### Colloidal stability:

To acquire the zeta capability of uncovered  $\text{Fe}_3\text{O}_4$ , Fe-Arg, and Fe-Arg-TMX, as demonstrated in Figure 5 was utilized DLS procedure. The surface charge influenced the colloidal solidness of Fe-Arg-TMX. It changed the zeta capability of Fe-Arg and Fe-Arg-TMX, though the exposed  $\text{Fe}_3\text{O}_4$  that affirmed the presence of arginine and TMX, individually. The zeta capability of uncovered  $\text{Fe}_3\text{O}_4$  was roughly  $-09.5$  mV that changed to  $+ 8.3$  mV after functionalization with arginine since the presence of amine utilitarian gatherings on the outside of Fe-Arg. Then again, the zeta possible changed to  $2.8$  mV after formation of TMX in view of the presence of carboxylic corrosive gatherings of it.

#### Thermal analysis:

To examine the warm conduct of Fe-Arg and Fe-Arg-TMX, TGA and DSC investigation was completed. TGA under  $\text{N}_2$  stream can be utilized to decide the weight percent of them. The example was warmed to  $600^\circ\text{C}$ . The measure of material lost because of warmth was gotten. The primary weight reduction beneath  $150^\circ\text{C}$  speaks to the expulsion of the retained water in the example. The weight reduction prior to joining TMX may be ascribed to the decline in L arginine covered on the Fe- Arg. After TMX formation, an extra weight reduction of Fe-Arg-TMX was seen which was come about because of complete debasement of natural mixes. At that point, DSC examination was utilized to consider uncovered iron notwithstanding Fe- Arg and Fe-Arg-TMX. The examples were warmed to  $300^\circ\text{C}$ . There were no endothermic and exothermic tops in uncovered iron up to  $300^\circ\text{C}$ .

Having been covered with Arg, its liquefying directs changed toward a lower temperature, affirming the covering of Fe-Arg. Liquefying purposes of Fe-Arg-TMX at  $172^\circ\text{C}$  demonstrated on endothermic pinnacle, while the softening purposes of Fe-Arg and TMX (information nat appeared) were shown at  $215.10$  and  $165.23^\circ\text{C}$ , individually. Along these lines, there was no unconjugated TMX in this item and since TMX was synthetically clung to MNPs, just one pinnacle was noticed.

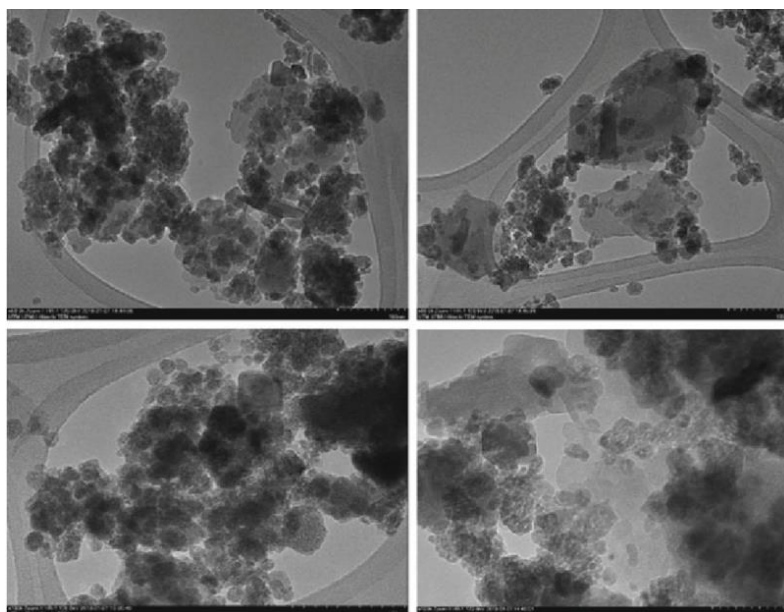


**Figure 6:** TEM image of Fe-Arg-TMX. TMX, Tamoxifen citrate; TEM, transmission electron microscopy

#### Drug release study:

Medication or Drug conjugation was planned as a system for delivering the medication into target cells. TMX was formed to Fe-Arg nanoparticles with a covalent bond. The peptide connection among TMX and Fe-Arg separated because of protease catalyst inside lysosomes under intracellular conditions. TMX was delivered into the objective cells and restrained dihydrofolatereductase chemical and halted the folic corrosive cycling that declined cell practicality. Fe-Arg-TMX nanoparticles with proteinase K chemical were brooded at low (pH = 5.4) like lysosomal conditions. TMX discharge was estimated by UV-Vis with absorbance at 235 nm. Studies were completed for 72 hr because of the continuation of the energy the arrival of TMX from Fe-Arg. The TMX discharge was seen before 12 hr span. In this examination, the medication discharge energy were explored in the nonappearance and presence of proteinase K. As seen, within the sight of the protein, about 62% TMX of Fe-Arg-TMX delivered after 12 hr, while without the catalyst, it was about 27%.

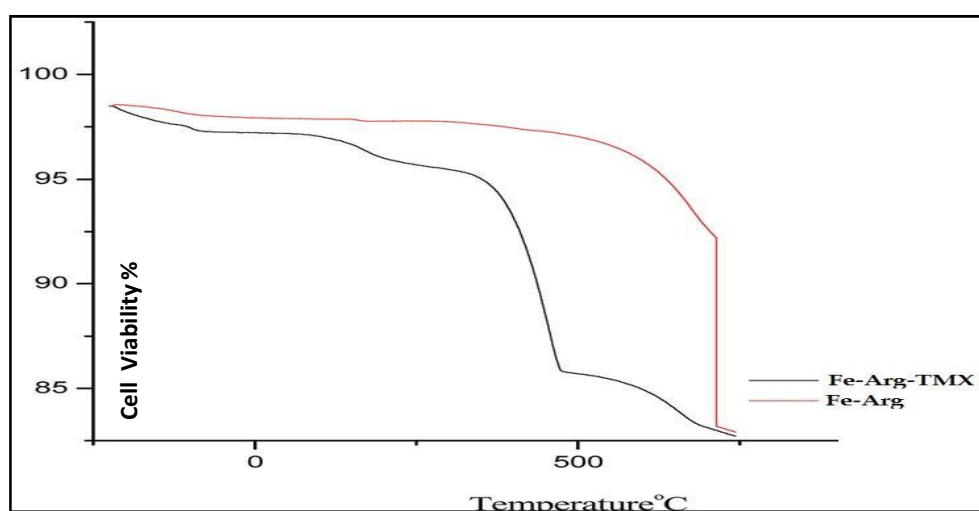


**Figure 7:** TGA curves of Fe-Arg and Fe-Arg-TMX. TMX, Tamoxifen citrate; TGA, thermogravimetric analysis

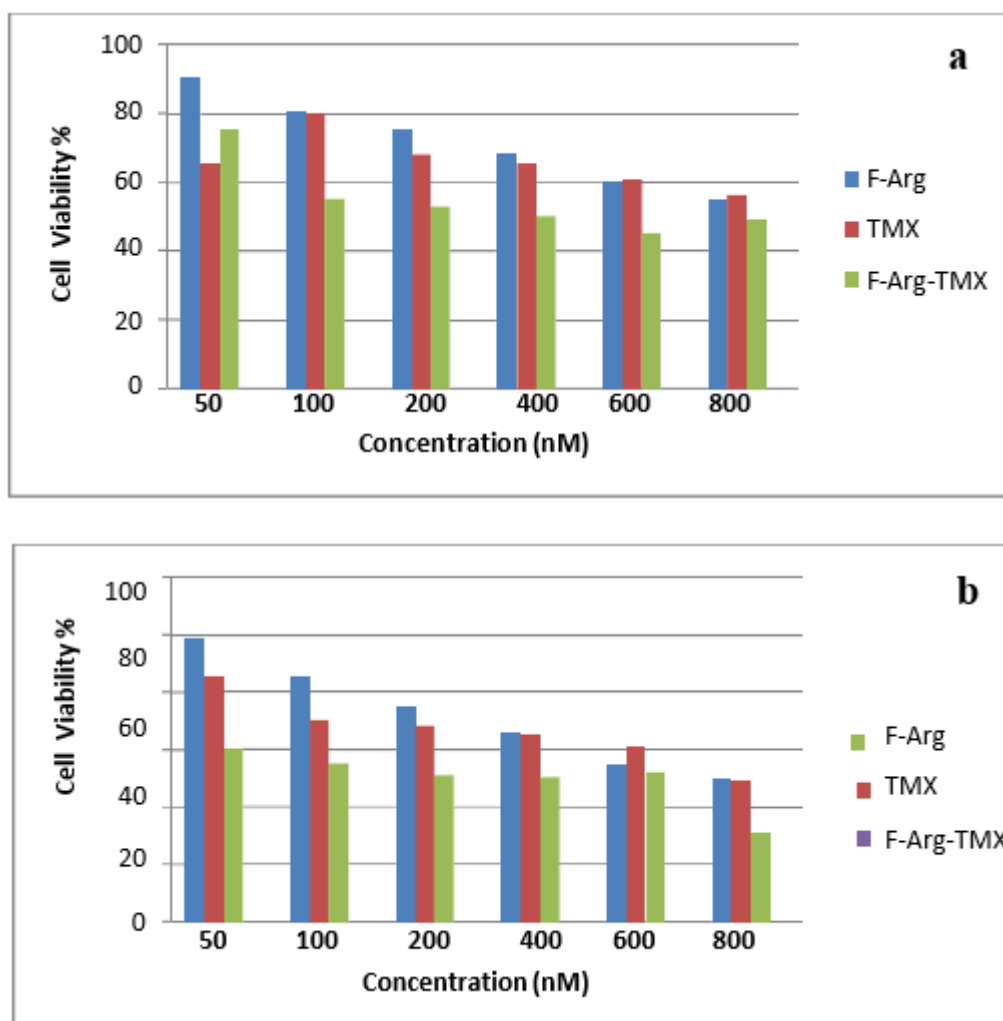


**Figure 8:** (a) Cytotoxicity analysis of free TMX, Fe-Arg, and (b) Fe-Arg-TMX after incubation for 48 hr and (b) 72 hr on HFF-2 cell line.

A lower thickness of Fe-Arg-TMX in correlation of free TMX was influenced more on malignant growth cells that demonstrated cleavage the TMX in the lysosomes. Along these lines, Fe-Arg-TMX NPs had higher cytotoxicity on bosom disease cell lines on account of controlled medication discharge. Subsequently, results diminished fundamentally.

### CONCLUSION:

FTIR results for Fe-Arg and Fe-Arg-TMX NPs were demonstrated in Figure 6.22 The pinnacles identified with carboxylic corrosive was seen in the scope of  $2,800\text{--}3,500\text{ cm}^{-1}$  in Fe-Arg-TMX, on the grounds that TMX has two carboxyl gatherings and one of the gatherings can be free. Aftereffects of VSM were demonstrated the lower estimation of the deliberate Ms of Fe-Arg and Fe-Arg-TMX than uncovered  $\text{Fe}_3\text{O}_4$  that was come about because of functionalization with arginine and formation with TMX, separately.

### REFERENCES:

1. Ali, I., Salim, K., Rather, M., Wani, W., & Haque, A. (2011). Advances in drugs for cancer chemotherapy. *Current Cancer Drug Targets*, 11(2), 135–146.
2. Ali, N., Rashid, S., Nafees, S., Hasan, S. K., & Sultana, S. (2014). Beneficial effects of chrysin against methotrexate-induced hepatotoxicity via attenuation of oxidative stress and apoptosis. *Molecular and Cellular Biochemistry*, 385(1–2), 215–223.
3. Chen, B., Wu, W., & Wang, X. (2011). Magnetic iron oxide nanoparticles for tumor-targeted therapy. *Current Cancer Drug Targets*, 11(2), 184–189.



4. Choi, G., Kim, T.-H., Oh, J.-M., & Choy, J.-H. (2018). Emerging nano materials with advanced drug delivery functions; focused on methotrexate delivery. *Coordination Chemistry Reviews*, 359, 32–51.
5. Choi, G., Kwon, O.-J., Oh, Y., Yun, C.-O., & Choy, J.-H. (2014). Inorganic nano vehicle targets tumor in an orthotopic breast cancer model. *Scientific Reports*, 4, 4430.
6. Dobson, J. (2006). Magnetic nanoparticles for drug delivery. *Drug Development Research*, 67(1), 55–60.
7. Gao, F., Yan, Z., Zhou, J., Cai, Y., & Tang, J. (2012). Methotrexate- conjugated magnetic nanoparticles for thermos chemotherapy and magnetic resonance imaging of tumor. *Journal of Nanoparticle Research*, 14(10), 1160.
8. Gupta, A. K., & Gupta, M. (2005). Synthesis and surface engineering of iron oxide nanoparticles for biomedical applications. *Biomaterials*, 26(18), 3995–4021.
9. Ke, X., & Shen, L. (2017). Molecular targeted therapy of cancer: The progress and future prospect. *Frontiers in Laboratory Medicine*, 1(2), 69–75.
10. Khan, Z. A., Tripathi, R., & Mishra, B. (2012). Methotrexate: A detail review on drug delivery and clinical aspects. *Expert Opinion on Drug Delivery*, 9(2), 151–169.
11. Kim, J.-E., Shin, J.-Y., & Cho, M.-H. (2012). Magnetic nanoparticles: of application for drug delivery and possible toxic effects. *Archives of Toxicology*, 86(5), 685–700.
12. Kimmick, G., Cirrincione, C., Duggan, D., Bhalla, K., Robert, N., Berry, D., Hudis, C. (2009). Fifteen-year median follow-up results after neo adjuvant doxorubicin, followed by mastectomy, followed by adjuvant cyclo phosphamide, methotrexate, and fluorouracil (CMF) followed by radiation for stage III breast cancer: A phase II trial (CALGB 8944).
13. *Breast Cancer Research and Treatment*, 113(3), 479–490. Kohler, N., Sun, C., Wang, J., & Zhang, M. (2005). Methotrexate- modified superparamagnetic nanoparticles and their intracellular uptake into human cancer cells. *Langmuir*, 21(19), 8858–8864.
14. Salimi, M. (2018). Comparative study of chemo-sensitivity expressed as micronuclei in lymphocytes of breast cancer patients, their un affected first degree relatives and normal controls as a possible prognostic marker. *International Journal of Radiation Research*, 16(1), 85–93.
15. Schwaminger, S. P., García, P. F., Merck, G. K., Bodensteiner, F. A., Heissler, S., Günther, S., & Berens meier, S. (2015). Nature of interactions of amino acids with bare magnetite nanoparticles. *The Journal of Physical Chemistry C*, 119(40), 23032–23041.
16. Shi, J., Votruba, A. R., Farokhzad, O. C., & Langer, R. (2010). Nano technology in drug delivery and tissue engineering: From discovery to applications. *Nano Letters*, 10(9), 3223–3230.
17. Singh, A., & Sahoo, S. K. (2014). Magnetic nanoparticles: A novel plat form for cancer the ranostics. *Drug Discovery Today*, 19(4), 474–481.
18. Ünal, B., Durmus, Z., Baykal, A., Sözeri, H., Toprak, M., & Alpsoy, L. (2010).
19. L-Histidine coated iron oxide nanoparticles: Synthesis, structural and conductivity characterization. *Journal of Alloys and Compounds*, 505(1), 172–178.
20. Viota, J., Arroyo, F., Delgado, A., & Horno, J. (2010). Electrokinetic characterization of magnetite nanoparticles functionalized with amino acids. *Journal of Colloid and Interface Science*, 344(1), 144–149.
21. Yu, S., & Chow, G. M. (2004). Carboxyl group (–CO<sub>2</sub>H) functionalized ferromagnetic iron oxide nanoparticles for potential bio-applications. *Journal of Materials Chemistry*, 14(18), 2781–2786.
22. Abolmaali, S. S., Tamaddon, A. M., & Dinarvand, R. (2013). A review of therapeutic challenges and achievements of methotrexate delivery systems for treatment of cancer and rheumatoid arthritis. *Cancer Chemotherapy and Pharmacology*, 71(5), 1115–1130